Contents lists available at ScienceDirect

Chemical Engineering Research and Design

journal homepage: www.elsevier.com/locate/cherd

Carbon capture and utilization via chemical looping dry reforming

Michelle Najera[b,c], *Rahul Solunke*[b], *Todd Gardner*[a], *Götz Veser*[a,b,c,*]

[a] *US DOE-National Energy Technology Laboratory, Pittsburgh, PA, United States*
[b] *Chemical Engineering Department, University of Pittsburgh, Pittsburgh, PA, United States*
[c] *Mascaro Center for Sustainable Innovation, University of Pittsburgh, Pittsburgh, PA, United States*

A B S T R A C T

Chemical looping combustion (CLC) is a clean energy technology for CO_2 capture that uses periodic oxidation and reduction of an oxygen carrier with air and a fuel, respectively, to achieve flameless combustion and yield sequestration-ready CO_2 streams. While CLC allows for highly efficient CO_2 capture, it does not, however, provide a solution for CO_2 sequestration.

Here, we propose chemical looping dry reforming (CLDR) as an alternative to CLC by replacing air with CO_2 as the oxidant. CLDR extends the chemical looping principle to achieve CO_2 reduction to CO, which opens a pathway to CO_2 utilization as an alternative to sequestration. The feasibility of CLDR is studied through thermodynamic screening calculations for oxygen carrier selection, synthesis and kinetic experiments of nanostructured carriers using cyclic thermogravimetric analysis (TGA) and fixed-bed reactor studies, and a brief model-based analysis of the thermal aspects of a fixed-bed CLDR process.

Overall, our results indicate that it is indeed possible to reduce CO_2 to CO with high reaction rates through the use of appropriately designed nanostructured carriers, and to integrate this reaction into a cyclic redox ("looping") process.

Keywords: Chemical looping; CO_2 utilization; Nanomaterials; Fixed bed reactors; Periodic reactor operation

1. Introduction

Carbon dioxide (CO_2) is widely recognized as the leading greenhouse gas (GHG) contributor to global warming. Among anthropogenic GHG emissions, combustion of fossil fuels is the leading cause of CO_2 emissions, constituting ~80% of the national U.S. GHG emissions from all sources on a CO_2 equivalent basis (U.S. E.P.A., 2010). Currently, the U.S. is deriving ~83% of total energy consumption from fossil fuels, and no significant change is anticipated for at least the next two decades (U.S. E.I.A., 2010). Worldwide trends mirror those in the U.S. closely. Hence, large global efforts are under way to develop efficient and affordable technologies to capture and sequester CO_2.

Among current CO_2 capture methods, chemical looping combustion (CLC) is a particularly promising emerging technology, which combines flameless NO_x-free combustion of fossil or renewable fuels with the efficient production of sequestration-ready CO_2 streams (Hossain and de Lasa, 2008; Ishida and Jin, 1994; Lyngfelt et al., 2001). In CLC, an oxygen carrier, typically a metal, is first oxidized with air in one reactor (oxidizer) and then reduced in contact with a fuel in a second reactor (reducer). The effluent of the reducer is a virtually pure mixture of CO_2 and steam so that following condensation of steam a high-pressure, sequestration-ready CO_2 stream is obtained (Ishida and Jin, 1994). However, while CLC is a highly efficient technology for CO_2 capture, it does not offer a solution for CO_2 sequestration. The lack of a secure and proven sequestration technology motivates efforts in our laboratory to develop alternate, chemical-looping derived process schemes, including the incorporation of CO_2 utilization within a CLC-based process.

* *Corresponding author at*: Chemical Engineering Department, University of Pittsburgh, 1249 Benedum Hall, Pittsburgh, PA 15261, United States.
E-mail address: gveser@pitt.edu (G. Veser).
Received 17 May 2010; Received in revised form 6 October 2010; Accepted 22 December 2010
0263-8762/$ – see front matter © 2011 The Institution of Chemical Engineers. Published by Elsevier B.V. All rights reserved.
doi:10.1016/j.cherd.2010.12.017

Nomenclature

C_P	heat capacity (J/kg K)
ΔH_R	heat of reaction (J/mol)
M_{act}	molecular weight of reactive component in solid carrier (kg/mol)
M_{CO_2}	molecular weight of CO_2 (kg/mol)
T_0	initial temperature (C)
T_{max}	maximum temperature (C)
ΔT_{max}	maximum temperature rise (C)
v_g	gas velocity (m/s)
v_h	heat front velocity (m/s)
v_r	reaction front velocity (m/s)
w_{act}	weight fraction of reactive component in solid carrier
w^{in}_{g,CO_2}	weight fraction of CO_2 in the feed
ρ	density (kg/m^3)
ε_s	porosity
ξ	stoichiometric factor (ratio of number of moles of gas to moles of solid in the oxidation reaction)

One alternative chemical looping process that has already been explored in some depth is chemical looping steam reforming (CLSR), which has been proposed as a means of H_2 production with integrated CO_2 capture by replacement of air with steam in the oxidizing reactor (Solunke and Veser, 2010; Takenaka et al., 2005; Zafar et al., 2006). Here, we propose chemical looping dry reforming (CLDR) as an alternate CLC process, in which CO_2 is used as an oxidant instead of air or steam. The CLDR configuration is shown in Fig. 1. Utilizing methane as a fuel, CLDR produces a net reaction similar to the dry reforming of methane as shown below where the stoichiometric half-reactions are based on a metallic 'M' oxygen carrier:

$$\text{oxidizer}: 4M + 4CO_2 \rightarrow 4MO + 4CO \quad \text{(R1)}$$

$$\text{reducer}: 4MO + CH_4 \rightarrow 4M + CO_2 + 2H_2O \quad \text{(R2)}$$

$$\text{netreaction}: CH_4 + 3CO_2 \rightarrow 4CO + 2H_2O \quad ((R3) = (R1) + (R2)) \quad \text{(R3)}$$

Dry reforming is one of the more established pathways for CO_2 utilization. For example, in typical methane dry reforming, methane (another greenhouse gas) and CO_2 are processed at elevated temperatures (>700 °C) over a catalyst (typically nickel or a noble metal) to produce syngas with a maximum H_2/CO ratio of 1 (Fan et al., 2009; Vernon et al., 1992) according to:

$$CH_4 + CO_2 \rightarrow 2CO + 2H_2 \quad \text{(R4)}$$

Typical challenges with current dry reforming technologies are catalyst cost and deactivation due to coking, as well as product selectivity for syngas (Choudhary and Choudhary, 2008; Moon et al., 2004).

The proposed CLDR process differs significantly from conventional catalytic dry reforming processes. While the target of conventional dry reforming is high syngas yield, CLDR results in fundamentally different stoichiometry (compare (R4) to (R3)), with the target of maximum CO yield and no selectivity for H_2 (assuming complete combustion of the fuel), i.e. CLDR yields a process which is optimized for CO_2 activation.

Another advantage of chemical looping dry reforming lies in its fuel flexibility. Chemical looping processes can, in principle, work with any fuel as long as the oxidized carrier shows sufficient reactivity with this fuel. CLC has to-date been demonstrated with methane (Mattisson et al., 2001; Ryden et al., 2008), synthesis gas (Mattisson et al., 2007), biofuels (Cao et al., 2006), and even direct coal feeds (Leion et al., 2007, 2009). In contrast, the catalyst in catalytic dry reforming is highly sensitive to the nature of the fuel, with coking and selectivity forming major obstacles for industrial realization of such processes.

Finally, CLDR can, in principle, handle dilute CO_2 streams as feed for the oxidizer (as long as the other feed gas components do not negatively interact with the carrier, i.e. as long as they are essentially chemically inert), while yielding a highly concentrated CO_2 stream at exit of the reducer. Therefore, CLDR can be conceptualized as a process that also concentrates dilute streams of CO_2.

In this contribution, we present results from a proof-of-concept study which aims to evaluate the potential of CLDR through a combination of thermodynamic calculations for carrier selection, synthesis and characterization of highly active and high-temperature stable nanostructured oxygen carriers,

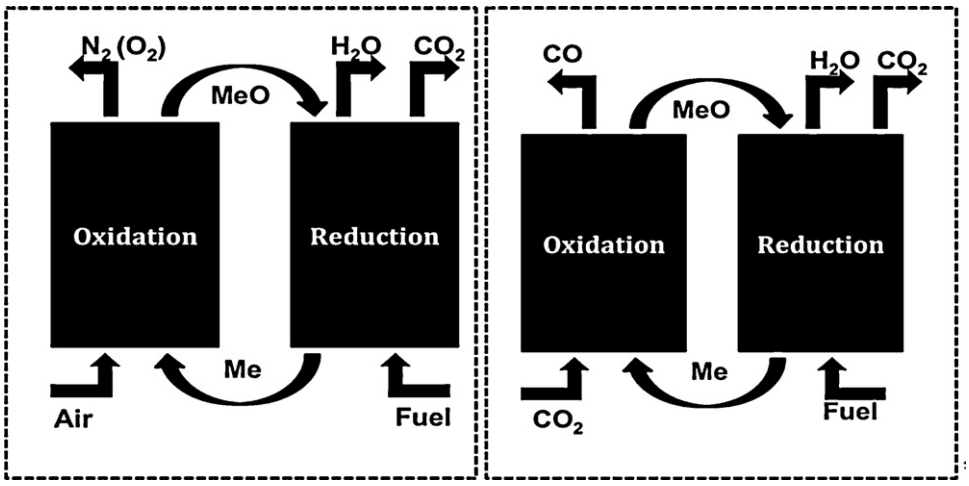

Fig. 1 – Schematic for (left) chemical looping combustion (CLC) and (right) chemical looping dry reforming (CLDR), shown with reduction of CO_2 to CO and full oxidation of a generic carbon-based fuel.

Table 1 – Screening results for CLDR carriers.

Carrier oxidation reaction	CO_2 carrying capacity (g CO_2/mol M)	Min. temp. (°C)	Max. temp. (°C)
$Mo + 2CO_2 \rightarrow MoO_2 + CO$	88	900	1000
$2Cr_3O_4 + CO_2 \rightarrow 3Cr_2O_3 + CO$	66	1700	2400
$3Fe + 4CO_2 \rightarrow Fe_3O_4 + 4CO$	59	700	1800
$Fe + CO_2 \rightarrow FeO + CO$	44	700	1800
$Zn + CO_2 \rightarrow ZnO + CO$	44	1200	1600
$Co + CO_2 \rightarrow CoO + CO$	44	200	300
$3FeO + CO_2 \rightarrow Fe_3O_4 + CO$	15	700	1800
$2NbO_2 + CO_2 \rightarrow Nb_2O_5 + CO$	11	1300	1500

and a brief reactor modeling study to evaluate process feasibility in a periodically operated fixed-bed reactor.

2. Results and discussion

2.1. *Thermodynamic screening of carriers*

A key issue in chemical looping processes is the selection of an appropriate oxygen carrier material. The reactivity of the carrier, its cost, toxicity, thermal stability, and attrition resistance (in the most common circulating fluidized bed reactor configuration for chemical looping) are critical selection criteria. For chemical looping reforming processes, reactivity is an even more stringent criterion than for conventional CLC, since the reactivity of H_2O or CO_2 as oxidants is significantly lower than for air (i.e., oxygen).

Thermodynamic screening calculations were conducted as a first step to identify suitable metals as active oxygen carrier components. A broad range of metals was analyzed using commercial software (FACTSAGE 5.0) to determine the thermodynamic equilibrium limitations for cyclic carrier oxidation and reduction in CLDR. This analysis performs a Gibbs free energy minimization of the reactant and product mixture at fixed temperature and pressure. To screen for suitable transition metal carrier materials, several factors were considered. Firstly, although a significant number of transition metals can be oxidized by CO_2, many of these same metals fail to exhibit suitable equilibrium conversion for the reduction reaction with a range of fuels. Additionally, suitable equilibrium conversion was often only achieved at temperatures nearing the melting points of the metals. Since CLC processes require stable oxygen carrier materials that can undergo extended high-temperature oxidation–reduction cycles with reproducible kinetics, materials that were only reactive above or near their melting points were eliminated. Lastly, cost and material toxicity were also considered in the selection.

Table 1 shows the results from CO_2 oxidation screening experiments for transition metals that were shown to have exhibited high thermodynamic carrier conversion (>20%) in both the forward and reverse reactions over a range of temperatures. The table lists the stoichiometric capacity for CO_2 reduction to CO in g CO_2 per mole of metal, which corresponds to the maximum reduction capacity in the absence of equilibrium limitations, in addition to the maximum and minimum reactor operating temperatures. The maximum temperature represents either the metal melting point, as is the case for Cr-, Mo-, Nb-based carriers, or the lowest temperature at which full conversion was achieved for reduction of the carrier with methane for Co-, Zn-, Fe-based carriers. The minimum temperature is defined as the temperature at which equilibrium conversion for carrier reduction with methane drops below 20%. The reduction temperature was selected as the minimum temperature determinant because the minimum temperatures required for sufficient carrier reduction were consistently higher than for carrier oxidation. The minimum and maximum temperatures given in Table 1 define the effective operating range for a CLDR process based on the respective carrier.

While a number of metals give reasonable CO_2 reduction capacity, it is apparent that only iron gives high oxygen storage capacity from CO_2 over a wide operating temperatures The very limited operating temperature range for Mo makes its use impractical, while Cr- and Nb-based carriers require temperatures well above those reasonable for reactor operation, and the very low temperature range for Co is prone to result in unacceptably slow kinetics. Iron-based carriers, which combine low cost, wide availability, and low toxicity, were thus selected for further analysis.

A general concern in CO_2 reduction processes is control of the degree of reduction. This is particularly true in any heterogeneously catalyzed CO_2 reduction process, or in a non-catalytic gas–solid reaction such as the presently considered oxidation of a metal carrier with CO_2. CO_2 reduction can result either in partial reduction to CO or deep reduction to elemental carbon (C). Since the formation of carbon can be expected to result in deposition and carrier deactivation due to active site occlusion, the reduction of CO_2 to C is undesirable. For this reason, the degree of CO_2 reduction, i.e. conversion and selectivity of the reduction process for the Fe-based carriers was studied. Fig. 2 shows the equilibrium CO_2 conversion in the case of stoichiometric CO_2 supply for the oxidation of Fe to FeO, Fe to Fe_3O_4, and FeO to Fe_3O_4, respectively, along with the corresponding selectivity to CO over a temperature range of 200–1000 °C. Clearly, while CO_2 conversion remains incomplete at all conditions, fairly high conversions (>50% for Fe and >30% for FeO) across the entire temperature range show again the wide operating range of iron-based carriers. These data demonstrate the process flexibility of iron as a carrier through the accessibility of three different oxidation states of iron with similar CO_2 conversion trends, albeit with different oxygen carrying capacities. It should be noted that the highest oxidation state of iron, Fe_2O_3, was not obtained as a thermodynamically accessible phase at any of the investigated conditions with CO_2 as oxidant, indicating the reduced oxidation capability of CO_2 in comparison to air.

The results in Fig. 2 show an almost step-wise change in selectivity of the CO_2 reduction from deep reduction to C at temperatures below ~500 °C to the desired reduction to CO at temperatures above ~700 °C which is independent of the initial and final states of the carrier. The thermodynamic results suggest that a chemical looping process for reduction of CO_2 to CO should be operated at temperatures above ~700 °C. The significance of this transition will be discussed further in relation to the reactivity of the nanostructured carriers (see Section 2.4).

Since incomplete carrier conversions were obtained at temperatures above ~700 °C, where carbon formation was thermodynamically unfavorable, further analysis was performed to test what excess (i.e., over-stoichiometric) feed of CO_2 would be required to shift the thermodynamic equilibrium in the CLDR oxidation reactor towards complete conversion of the carrier to Fe_3O_4. The calculations were performed for Fe as well as FeO as starting points of the oxidation, since previous studies have shown that for some fuels com-

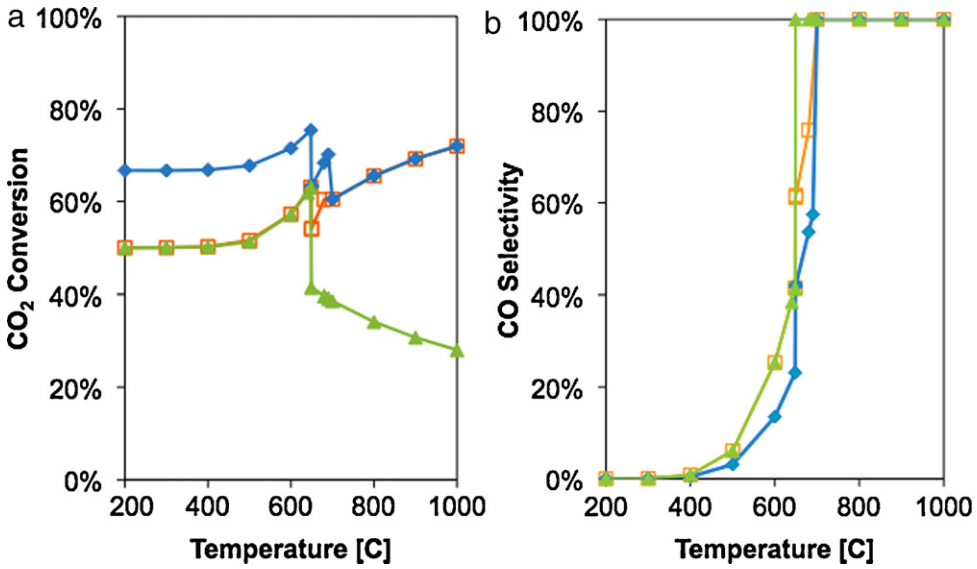

Fig. 2 – Thermodynamic calculations with CO_2 conversion (left) for oxidation of Fe to Fe_3O_4 (open squares), Fe to FeO (diamonds), and FeO to Fe_3O_4 (triangles) with stoichiometric amount of CO_2 for corresponding metal oxidation and reduction to CO, and reaction selectivity (right) for reduction to CO for Fe to Fe_3O_4 (open squares), Fe to FeO (diamonds), and FeO to Fe_3O_4 (triangles), demonstrating shift in selectivity for CO_2 reduction to CO between ~500 and 700 °C.

plete reduction to Fe is not achievable and FeO represents the lowest accessible oxidation state in the chemical looping process (Mattisson et al., 2001). Here, we define excess CO_2 as the percentage of CO_2 required beyond the stoichiometric requirement to form Fe_3O_4. "0% excess" therefore, represents full conversion to Fe_3O_4 with a stoichiometric feed of CO_2, while 100% excess indicates a twofold stoichiometric supply of CO_2. Results are shown in Fig. 3 as a function of temperature in the high-temperature range above ~650 °C where complete selectivity for CO is attained.

One can see that large excess of CO_2, ranging from ~150 to 200% excess, is required to attain full conversion of Fe to Fe_3O_4, while much more moderate values of <30% excess are obtained for the conversion of FeO to Fe_3O_4. Thus, although less CO_2 is reduced per mol of iron in the case of oxidation of FeO to Fe_3O_4, this configuration would be more practical for reactor operation, since high conversion could be achieved with low excess amounts of CO_2. It should be mentioned, however, that the thermodynamic calculations are based on the assumption of a closed system, i.e. they mimic the behavior of a reactor system in which the gas and solid phase are co-moving through the reactor at an identical speed. Careful choice of a suitable reactor configuration, such as counter-current gas and solid phases or a fixed-bed reactor, would result in gas–solid contacting patterns in which the carrier is brought into contact with a continuously "refreshed" gas phase, allowing the reaction to continually shift towards product formation. Such a configuration would hence mimic the situation in a closed system with strongly over-stoichiometric gas supply (i.e. the configuration for the calculations in Fig. 3) without actually requiring the excess gas feed.

In order to assess the thermodynamic limits during the carrier reduction with fuel, similar equilibrium calculations were conducted for the reduction reaction using methane as the fuel in the reducer. Fig. 4 shows the result of these calculations for reduction of Fe_3O_4 in methane over a range of temperatures from 600 to 1400 °C (since the thermodynamic

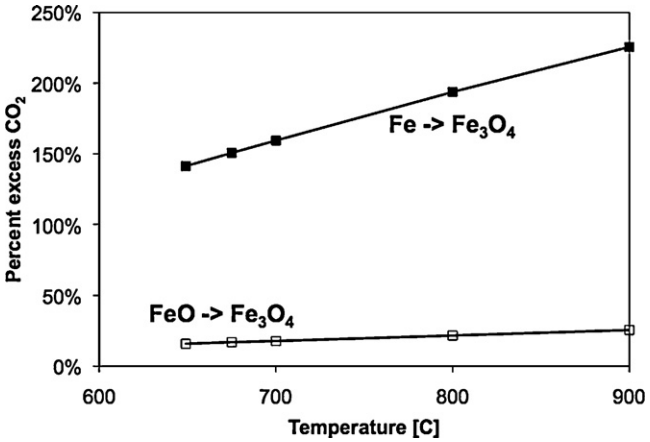

Fig. 3 – Stoichiometric excess of CO_2 (for reduction to CO) required for complete conversion of Fe (filled squares) and FeO (open squares) to Fe_3O_4 for temperatures between 650 and 900 °C.

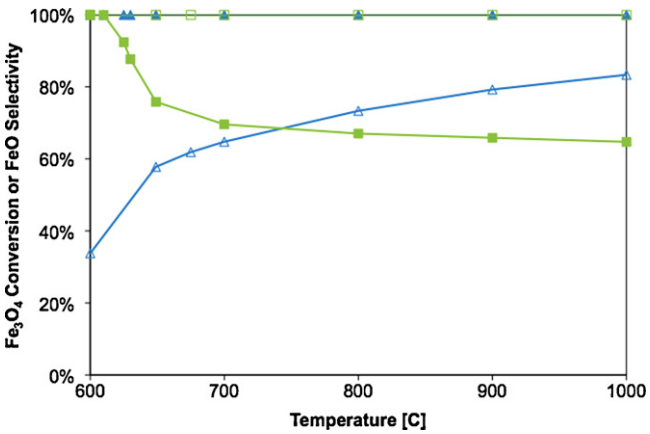

Fig. 4 – Thermodynamic calculations for carrier reduction with stoichiometric supply of methane for reduction of Fe_3O_4 to FeO (open symbols) or Fe (filled symbols), respectively. Shown are Fe_3O_4 conversion (triangles) and selectivity to FeO (squares). Increasing methane supply results in increased conversion and deeper reduction of the carrier.

calculations for oxidation of Fe or FeO with CO_2 indicated that Fe_2O_3 was not a product in this process, Fe_2O_3 was not considered from these calculations). For reduction of the carrier with methane, two different pathways need to be considered: Methane can either be combusted to CO_2 and H_2O, or partially oxidized to CO and H_2 (syngas). The respective reactions are shown below for Fe_3O_4 as the oxidized carrier state and FeO or Fe as the reduced state, respectively. The calculations in Fig. 4 are based on a stoichiometric feed of methane for the total oxidation of methane, and FeO and Fe as a reduced state of the carrier, i.e. the two stoichiometric feeds considered correspond to the two combustion reaction stoichiometries shown below:

$$\text{Combustion, FeOasreducedstate}: CH_4 + 4Fe_3O_4 \rightarrow CO_2 + 2H_2O + 12FeO$$

$$\text{Combustion, Feasreducedstate}: CH_4 + Fe_3O_4 \rightarrow CO_2 + 2H_2O + 3Fe$$

$$\text{Partialoxidation, FeOasreducedstate}: CH_4 + Fe_3O_4 \rightarrow CO + 2H_2 + 3FeO$$

$$\text{Partialoxidation, Feasreducedstate}: CH_4 + 0.25Fe_3O_4 \rightarrow CO + 2H_2 + 0.75Fe$$

The results show that the targeted reduction of Fe_3O_4 to FeO with stoichiometric methane supply results in increasing conversion with increasing temperature, with conversions >60% at temperatures above ~700 °C. In this case, FeO is the only reduction product for the carrier (i.e. $S_{FeO} = 100\%$ at all temperatures). Conversely, supplying sufficient methane for stoichiometric reduction of Fe_3O_4 to Fe results in full carrier conversion at all temperatures, with a mixture of FeO and Fe as reduction products and >60% selectivity towards FeO. Finally, calculations based on FeO as the starting material and again stoichiometric supply of methane for total oxidation (not shown) results in conversions below ~35% over all temperatures, with zero-valence Fe as the only accessible reduction state. Overall, these calculations indicate that the most efficient CLDR process with methane as the fuel will operate between Fe_3O_4 and FeO as upper and lower oxidation state of the carrier, respectively.

The incomplete conversions and selectivities, respectively, in Fig. 4 indicate that the reaction pathway in methane oxidation over iron oxides can be expected to be a mix of total and partial oxidation. In the presently proposed process, total oxidation would be the preferred reaction pathway in order to maximize the reduction potential of the methane feed and to obtain a pure CO_2/steam mix at the exit of the oxidizer from which sequestration-ready CO_2 streams could be obtained via steam condensation.

In order to further quantify methane oxidation products, Fig. 5 shows the gas phase conversion and selectivity for Fe_3O_4 reacting with methane at the stoichiometric ratio for total oxidation. Although the overall conversion of methane is very high (>95%) across the entire temperature range, the observed values for selectivity are poor. Selectivity for total oxidation products increases from ~20% at 900 °C to up to ~60% at 650 °C. This result is holds regardless of stoichiometry for full or partial oxidation of methane (with a slight increase in selectivity for partial oxidation products with an increase methane feed),

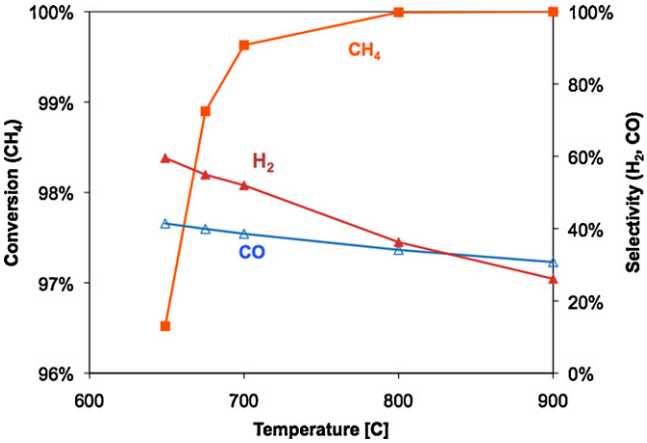

Fig. 5 – Methane conversion (squares) with stoichiometric methane feed for full oxidation with oxidized carrier Fe_3O_4, showing temperature dependent selectivity of partial oxidation over full oxidation (H_2 over H_2O (open triangles) and CO over CO_2 (filled triangles)).

and points out a limitation of operating a CLDR process with methane as the fuel. Additionally, calculations showed that carbon formation is also predicted in the reduction reactor for temperatures below 650 °C for Fe_3O_4 reduction with a stoichiometric methane supply. However, we have previously shown that syngas as fuel, for example, allows essentially complete conversion, indicating that alternate fuels might give more encouraging results (Solunke and Veser, 2009). The proper reactor flow configuration, as discussed above for the carrier oxidation with CO_2, can give rise to a gas–solid contact pattern which results in an effective over-stoichiometric supply of either of the reactants and hence in higher conversions than those predicted from closed system equilibrium calculations.

Overall, the thermodynamic screening calculations showed that Fe-based carriers are, despite some shortcomings, the most promising carrier materials, and Fe was hence chosen for subsequent experimental investigations.

2.2. *Experimental*

Based on the thermodynamic analysis, which had indicated that iron is the most promising carrier material for a CLDR process, nanostructured iron carriers were synthesized for experimental evaluation of the CLDR process. The nanostructuring of the carrier was chosen since CO_2, as a weak oxidant, is likely to result in slow oxidation kinetics and we had previously shown that nanostructuring can result in highly active and stable oxygen carriers in CLC. (Kirchhoff et al., 2005; Solunke and Veser, 2009). Iron-based carriers were synthesized, characterized, and evaluated in thermogravimetric analysis (TGA) and fixed-bed reactor tests.

2.3. *Synthesis and characterization*

One obvious challenge with this work stems from the stability and low free energy of the CO_2 molecule and its correspondingly low activity as an oxidant, in particular when compared to air. Ideally, any CLC carrier should exhibit fast and stable reaction kinetics in addition to facilitating complete redox reactions in order to enable high reactor throughput and minimize or completely avoid downstream gas separation requirements. While the oxidation of iron-based materials with CO_2 has previously been reported in the literature, the

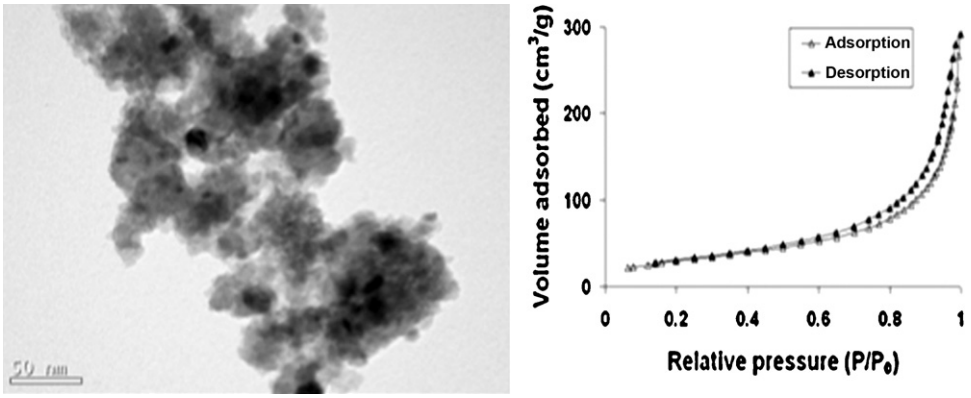

Fig. 6 – Typical Fe-BHA sample showing 15–20 nm iron particles (dark) surrounded by barium hexa-aluminate support (grey) (left); and nitrogen sorption isotherm (right).

reported rates are low and indicate the need for a suitable carrier formulation to accelerate the reaction (Tamaura and Tabata, 1990; Akanuma et al., 1993; Yamasue et al., 2007). As to the reduction reaction, iron has previously been evaluated as a carrier in CLC for methane combustion, showing that the reduction half-reaction of the CLDR loop should be achievable with an iron-based material (Mattisson et al., 2001). However, iron oxides are well known to form dense oxide over-layers which severely slow down the oxidation kinetics and limit accessibility of bulk iron. Furthermore, due to the high-temperature conditions of chemical looping processes, high-temperature stability, i.e. strong resistance to sintering, is a significant concern.

We have previously shown that nanostructuring can result in highly stable and active catalysts and oxygen carriers (Kirchhoff et al., 2005; Solunke and Veser, 2009), and applied the same approach here towards the synthesis of nanostructured Fe–BHA (BHA = barium hexaaluminate) oxygen carriers.

The synthesis is based on a reverse microemulsion-templated sol–gel process in which metal nanoparticles are synthesized simultaneously with a ceramic matrix via a one-pot approach (Kirchhoff et al., 2005). An aqueous metal salt solution of $(Fe(NO_3)_3{\cdot}9H_2O$ (99.999%) is mixed with iso-octane (2,2,4-trimethylpentane, 99.7%), a surfactant (poly(ethylene oxide)-*block*-poly(propylene oxide)-*block*-poly(ethylene oxide), Aldrich) and a co-surfactant (1-pentanol (99+%)). Aluminum isopropoxide and barium isopropoxide (both 99.9%) are dissolved at a stoichiometric ratio of 1–12 under inert gas as precursors of barium hexaaluminate (BHA), a high temperature stabilized alumina (Inoue et al., 1997). The isopropoxides are then added to the reverse microemulsion where they migrate into the water micelles and hydrolyze. In parallel, the metal salt forms metal nanoparticles, which remain embedded in the porous BHA framework. The reverse microemulsion is aged for ~48 h, and then separated by temperature-induced phase separation. The product phase undergoes several washing steps with acetone, followed by volatile removal via freeze-drying. The final product consists of a dry powder, which is calcined for 5 h at 500–900 °C to generate the final carrier material.

The nanostructured carriers were characterized by X-ray diffraction (XRD), nitrogen sorption (BET), and transmission electron spectroscopy (TEM, JEOL 200). A typical TEM image of calcined material is shown in Fig. 6 (left), where Fe particles of 15–20 nm size are surrounded by an amorphous BHA matrix. The N_2 adsorption isotherm shown in Fig. 6 (right) shows a typical hysteresis corresponding to type-IV mesoporous material with a broad pore distribution, with pore sizes between 10 and 50 nm, that facilitate access to the active carrier material by the reactive gases. BET surface areas after calcination at 600 °C between 100 and 150 m^2/g. All carriers used in the present study had a weight loading of 40 wt% Fe.

2.4. *Reactive tests*

To test the reactivity of these nanostructured Fe–BHA carrier materials, thermogravimetric analysis (TGA) and fixed-bed reactor studies were conducted using hydrogen as a model fuel. This fuel was chosen to avoid complications due to competition between partial vs. total oxidation pathways when using methane as fuel (as identified in the thermodynamic analysis above), and hence to focus on the oxidation of the carrier using CO_2 as an oxidant as well as on the stability of the carrier in cyclic redox operation. Coincidentally, using hydrogen as fuel in CLDR results effectively in reverse water–gas shift (RWGS) as net reaction: $CO_2 + H_2 = CO_2 + H_2O$. While this reaction is of some industrial interest, the use of hydrogen is based entirely on the fact that it is a convenient, highly reactive model fuel with a single oxidation pathway.

Initial reactivity tests consisted of thermogravimetric analysis (TGA) of Fe–BHA material with CO_2 as the oxidant, H_2 as the reducing gas, and an Ar gas purge phase between oxidation and reduction phases. It should be noted that unlike for CLC, where the purge phase is critical in order to avoid uncontrolled mixing of oxygen with fuel upon switching between oxidation and reduction phases, CLDR does not require such a purge phase and it is added in the experiments purely for the purpose of attaining separated gas phase signals from each half-cycle.

Fig. 7 shows the sample weight versus time during oxidation of a 40 wt% Fe–BHA carrier sample at three temperatures (600, 700, and 800 °C). One can see that the reduced and oxidized sample weights (i.e. lowest and highest sample weights, respectively) agree within experimental error between all three experiments, indicating that the same degree of conversion is achieved in all cases. Furthermore, the sample weight increases initially very rapidly, and then slows down before reaching the final value. This is particularly pronounced at the lower two temperatures, while the kinetics at the highest temperature of 800 °C show a much faster, almost step-wise transition from the reduced to the oxidized state within ~2 to 3 min.

Carrier conversion in TGA can be defined as $X = (M_t - M_{red})/(M_{ox} - M_{red})$, where M_t represents the sample

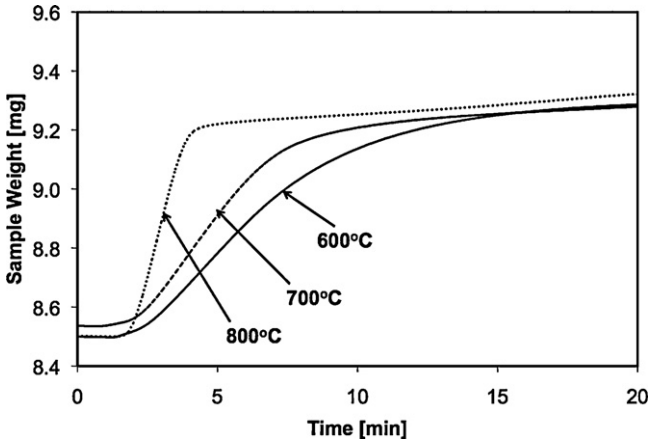

Fig. 7 – Time traces for oxidation of 40 wt% Fe–BHA with CO_2 at three different temperatures in TGA.

mass at time t, M_{red} is the mass of the fully reduced sample, and M_{ox} the mass of the fully oxidized sample. Hence, $X = 0$ corresponds to the fully reduced carrier and $X = 1$ corresponds to a fully oxidized carrier. This renormalizes the above curves, and allows calculation of a conversion rate, dX/dt, by computing the time derivative of the conversion time traces.

Fig. 8 shows the results of these calculations as rate dX/dt versus time t. Again, the fast initial rate of oxidation is apparent with a subsequent slow-down of the oxidation rate. Strikingly, however, the rate is only mildly increased upon raising the temperature from 600 to 700 °C, and then shows a very strong increase from 700 to 800 °C. It is interesting to review this observation in connection with the thermodynamic calculations given in Fig. 2. The temperature range between 600 and 800 °C corresponds to a range where thermodynamics predicts a transition in the selectivity of the oxidation reaction from carbon to CO as the main product. Thus, the transition to the much faster oxidation at 800 °C may be associated with this switch in the reaction path, either because the reduction of CO to C is much slower than the first oxygen abstraction such that overall carrier oxidation is slower, or because the formation of carbon at lower temperatures results in carbonaceous residues on the sample surface that leads to an overall slower reaction due to mass transfer limitations. The observations from the fixed-bed reactor experiments discussed below suggest that small amounts of carbonaceous deposits are indeed present, supporting the second explanation. However, the fact that the sample weight is essentially unchanged with temperature indicates that the amount of these carbon deposits must be small.

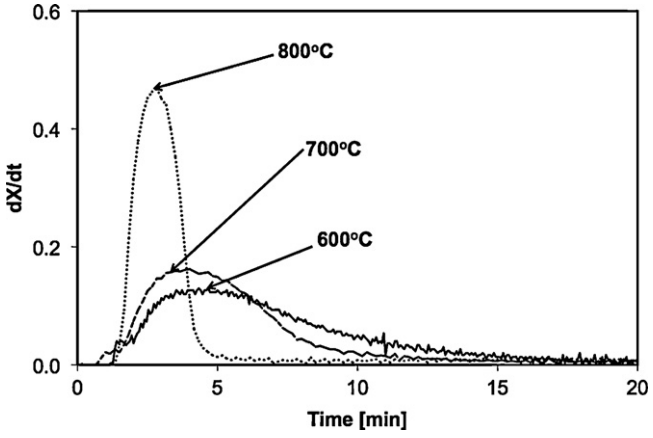

Fig. 8 – Reaction rates during oxidation of a 40 wt% Fe–BHA carrier sample with CO_2 for temperatures 600–800 °C, as calculated from the data in Fig. 7.

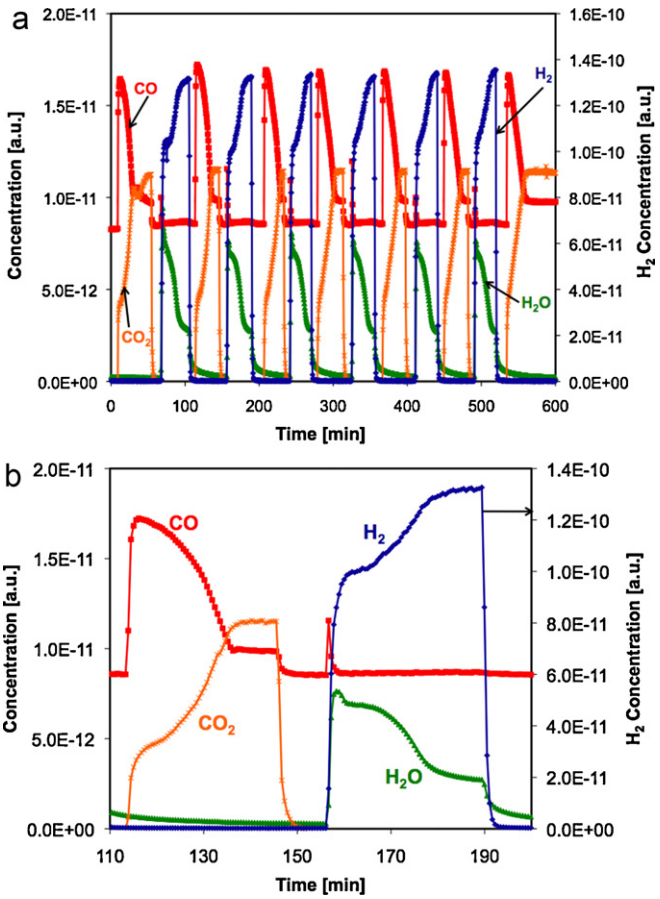

Fig. 9 – Fixed-bed reactor cycles (top graph) and single cycle (bottom graph) at 700 °C with Fe–BHA oxidation in CO_2 and reduction in H_2 (as a model fuel, on separate axis), showing chemical looping operation resulting in RWGS reaction and demonstrating stable operation for CO_2 carrier oxidation.

Following the cyclic TGA experiments, the Fe–BHA samples were subjected to cyclic reduction–oxidation in a fixed bed reactor configuration. 220 mg of Fe–BHA were loaded into a quartz–glass tube (1/4″ I.D.) and placed horizontally in an electric oven. This system was heated to 700 °C in Ar and then alternating phases of H_2 and CO_2 were contacted with the Fe-based carrier at a flow rate of 5 sccm at 700 °C for six ~30 min oxidation and reduction cycles. Reduction and oxidation half-cycles were again separated by an Ar purge phase. The product gases were monitored via mass spectrometry (Pfeiffer Omnistar QMS 200).

Fig. 9 shows all 6 cycles along with a more detailed breakout of a single cycle. The results show stable cyclic operation of the carrier as apparent from the unchanged product gas traces for the entire duration of the experiment (~10 h). Review of a single cycle shows a fast onset of CO formation in the reactor effluent as a result of CO_2 reduction during the oxidation half-cycle, followed by a slow decay for the CO signal over the next ~20 min of operation. Similarly, CO_2 conversion is very high (>90%) over the first ~10 min of the oxidation phase, and then decreases in parallel with the decreasing CO formation. Clearly, in order to attain high CO yields, the oxidation phase should be stopped after ~10 min of operation and the reactor should be switched to the reduction phase.

During the reduction half-cycle, one can see similar trends as during oxidation: a very fast onset of H_2O formation indicates fast reduction of the carrier, transitioning to slower reduction after ~15 min, i.e. halfway through the cycle. Interestingly, continued water formation indicates that even after 30 min, i.e. at the end of the reduction half-cycle, the carrier is not yet completely reduced. Hydrogen conversion remains incomplete at all times throughout the reduction half-cycle, indicating that slower flow rates, i.e. increased contact times, would be preferable for efficient reactor operation. By limiting the oxidation and reduction half-cycles to the first ~10 min each, and by adjusting the feed flow rates, CO yields and H_2 conversion could potentially be maximized, however, at the expense of carrier utilization.

Finally, a small, but reproducible, CO pulse at the very onset of the reduction cycle indicates the presence of a small amount of carbon on the sample, which is gasified by the steam formed during carrier reduction. This is in agreement with the interpretation of the TGA experiments, discussed above, as well as with the results of the thermodynamic analysis indicating that 700 °C is roughly the upper temperature range at which carbon formation must be expected.

Overall, the TGA and fixed-bed reactor experiments indicate that CLDR with Fe-based carriers could potentially be a feasible process. However, the relatively low reactivity of both CO_2 as well as Fe, and the potential for carbon formation will require careful design and operation of such a process.

2.5. *Fixed bed reactor calculations*

The most commonly discussed reactor configuration for chemical looping processes is a two-reactor circulating fluidized bed (CFB) configuration. Although CFB operation is known to provide excellent heat and mass transfer characteristics, which are critical for CLC, CFBs also present significant operational challenges with regard to oxygen carrier transport and particle attrition (Lyngfelt et al., 2001). Alternatively, CLC operation in a cyclically operated fixed bed reactor (FBR) has also been proposed, although heat management is a problem in this case (Noorman et al., 2007). However, in chemical looping reforming processes, the heat of the carrier oxidation reaction is substantially reduced, therefore reducing the probability of obtaining hot spot formation in the fixed bed, and unacceptable temperature maxima in the cyclic operation of the reactor. In fact, since dry reforming is overall endothermic, the use of a FBR system is expected to be advantageous since the heat generated from the exothermic oxidation half-cycle is regeneratively transferred via the oxygen carrier to the subsequent endothermic reduction step, resulting in highly efficient heat integration between the two half cycles (Neumann and Veser, 2005; Liu et al., 2009; Veser, 2010). Indeed, heat integration through the use of periodically operated fixed bed reactor systems for endothermic reactions has been previously proposed by others, for counter-current flow, and has been shown to result in super adiabatic temperatures at autothermal conditions (Glockler et al., 2004; Kolios et al., 2000).

Here, we consider a simple fixed-bed reactor operation in which the bed is operated periodically between oxidation with CO_2 and reduction with methane in a co-current configuration, giving rise to traveling gas and temperature waves through the reactor. Such a configuration entirely avoids carrier attrition and separation issues, which form the main concern in current CFB CLC process development, but the thermal dynamics of the system requires consideration in order to avoid unacceptable maximum temperatures.

A simplified heat and mass transfer model for CLDR operations is analyzed in the following. The model was originally developed by Kuipers and coworkers for conventional CLC (Noorman et al., 2007), and later adapted by Solunke and Veser (2010) for chemical looping steam reforming (CLSR). The calculations presented here are based on a dynamic analysis of the pseudo-homogeneous energy balance for a fixed-bed CLC process. Noorman et al. demonstrated that this energy balance can be solved analytically given several simplifying assumptions. Here we will briefly review the model derivation by Kuipers and coworkers, adapted for our dry reforming process. The maximum temperature excursions in the bed can be directly derived from the energy balance given the following assumptions: it is assumed that the carrier in the fixed-bed is initially in its reduced form (FeO), and reacts with the CO_2 instantaneously, i.e. with an infinitely fast reaction rate, until complete carrier conversion is attained. Similarly, instantaneous, complete reaction of Fe_3O_4 with methane during for the reduction phase is assumed. While neither assumption (infinite reaction rate or complete conversion) is strictly true in our case, as seen in the thermodynamic calculations and reactor experiments above, the analysis based on these assumptions will yield a worst-case estimate for the maximum temperatures that can be expected in the process.

The coupling between the gas–solid reaction and the convective gas flow results in the formation of two spatially separated travelling wave fronts which move through the reactor with different front velocities. Assuming all of the heat within the solid material is transferred to the gas phase at the heat front and all CO_2 in the feed reacts instantaneously with the solid carrier, these front velocities are given as:

$$v_h = \frac{\rho_g v_g C_{p,g}}{\varepsilon \rho_s C_{p,s}} \tag{1}$$

and

$$v_r = \frac{\rho_g v_g w^{in}_{g,CO_2} M_{act}}{\varepsilon_s \rho_s w_{act} M_{CO_2} \xi} \tag{2}$$

(for the meaning of the variables please see section 'Nomenclature'). The first is the velocity of the heat front (v_h), and the second is the velocity of the reaction front (v_r), where the oxidant (CO_2) reacts with the reduced oxygen carrier (FeO). It is assumed that the heat capacity of the gas and the solid ($C_{P,g}$ and $C_{P,s}$) and the solid density (ρ_S) are constant, and that the influence of pressure drop over the fixed bed and the variation of the mass flow rate can be neglected. Since the heat capacity of the reactants ($C_{P,g}$) is only weakly dependent on temperature over the temperature range of interest, an average value $C_{P,g}$ was utilized and the calculations are not dependent on a specific reference temperature.

Assuming furthermore that the gas phase volumetric heat capacity is negligible, the heat produced by the oxidation of the oxygen carrier is taken up entirely by the solid carrier, and the energy balance can then be written as

$$\frac{\rho_g v_g w^{in}_{g,CO_2}}{M_{CO_2}} (-\Delta H_R) = \varepsilon_s \rho_s C_{P,s} (v_r - v_h)(T_{max} - T_0) \tag{3}$$

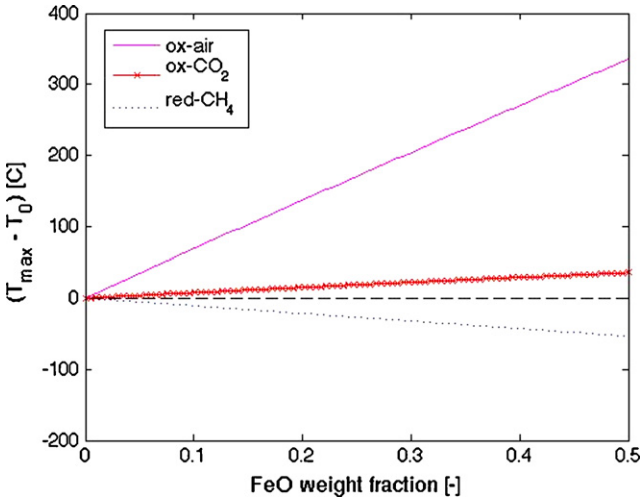

Fig. 10 – Maximum temperature change in FBR during reduction with oxidation with air and CO_2 and reduction with methane or H_2 as function of the weight fraction of active component (FeO) in the carrier.

Combining Eqs. (1) and (2) into (3) and gives the maximum temperature rise in the bed:

$$\Delta T_{max} = (T_{max} - T_0) = \frac{-\Delta H_R}{(C_{P,s}M_{act}/w_{act}\xi) - (C_{P,g}M_{CO_2}/w^{in}_{g,CO_2})} \quad (4)$$

As already pointed out by Noorman et al., the maximum temperature rise is independent of the gas flow velocity, due to the assumption that the heat capacity of the gas phase is small in comparison to the solid phase, which results in negligible convective heat transport with the gas flow. Furthermore, Eq. (4) does not account for the influence of the reaction rate on the maximum temperature rise, which is a result of the assumption of an essentially instantaneous reaction and will hold as long as the reaction rate is sufficiently fast (Noorman et al., 2007). While the incomplete conversions observed in our experiments will result in significant dampening of the temperature maxima as compared to the model results, the fast onset of the reactions and high reaction rates, particularly during the first phase of reduction and oxidation, respectively, can be expected to satisfy the present assumption. Lastly, in agreement with our thermodynamic analysis above, FeO was assumed as the reduced state of the carrier and Fe_3O_4 as the oxidized state.

Fig. 10 shows the maximum temperature change during the reduction of a iron-based carrier with methane as fuel along with the maximum temperature rise during oxidation of the carrier with CO_2 and, for comparison, with air as a function of the weight fraction of FeO in the oxygen carrier. As expected, the maximum temperature rise in the reactor during carrier oxidation is dramatically lowered upon switching from air to CO_2 as oxidant. While temperature maxima for oxidation with air exceeds 300 °C, the temperature rise during oxidation with CO_2 never increases above 50 °C. Clearly, hot spots or temperature peaks are unlikely to pose a concern in a fixed-bed CLDR process.

In fact, the temperature maxima in Fig. 10 illustrate another important aspect of CLDR. Since the process yields methane dry reforming as overall reaction, it is a strongly endothermic process, as apparent in the fact that the temperature minima in the oxidizer exceed the maxima in the reducer (in terms of absolute values). In practice, the process could be operated via externally fired reactors, as done in industrial steam reforming of methane. However, this would counter the intent of the process as a net CO_2 consumer, since this combustion process would again result in CO_2 emissions. Alternatively, the process could be rendered autothermal by co-feeding oxygen with CO_2 as co-oxidizer, in close analogy to industrial autothermal methane reforming (Rostrup-Nielsen, 2002). The overall reaction hence would give:

$$CH_4 + yCO_2 + (3-y)/2O_2 \rightarrow (1+y)CO + 2H_2O$$

A thermodynamic analysis yields $y = 1.83$ in order to attain a thermo-neutral reaction, i.e. in practice the process would require slightly lower values of y in order to attain a mildly exothermal process for autothermal operation.

In CLDR, several alternate schemes for this oxygen co-feed are possible: The oxygen could be directly co-fed with CO_2 to the oxidizer, or it could be fed with methane to the reducer. Clearly, the latter is the more favorable configuration, since it reduces the endothermicity of the reducer reaction, which minimizes the temperature swing between the oxidation and reduction half-cycles. Since the required methane/oxygen mixture would be well above the fuel-rich flammability limit, process safety would not be a significant concern. Furthermore, co-feeding oxygen with methane would allow an increase in fuel conversion and improve selectivity towards total oxidation products while aiding in removing any potential carbon residues, i.e. it would help to overcome some of the issues identified above in our thermodynamic analysis and in the reactor experiments.

As for the oxygen source, oxygen could either be fed as air or as a pure O_2 stream. Feeding air would be preferable from a cost perspective. However, it would result in a strong dilution of the CO_2 stream from the reducer with ~70 vol% N_2 after steam condensation (assuming complete conversion of methane to total oxidation products), counter-acting the intent of the process to yield sequestration-ready CO_2 streams on the reducer side. Hence, efficient process operation would require a purified oxygen feed at the expense of process operating cost.

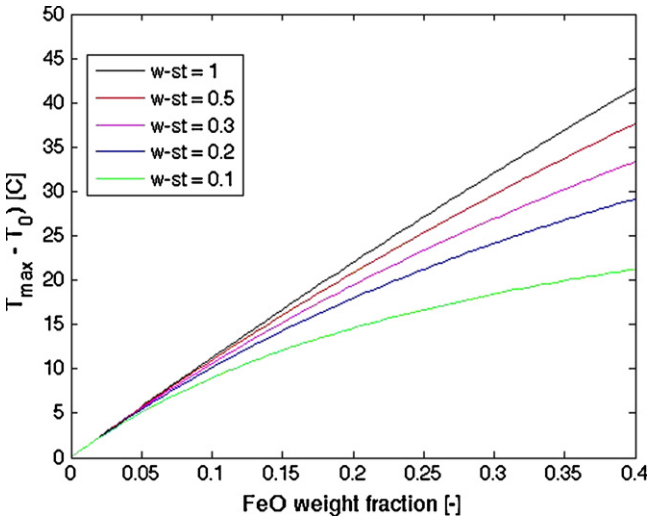

Fig. 11 – Maximum temperature increase in a fixed-bed reactor during oxidation with CO_2 vs. FeO loading of the carrier, showing the effect of CO_2 weight fraction in the reactor feed.

As previously discussed, the operation of CLDR with dilute CO_2 streams also poses an intriguing possibility for utilization of such dilute CO_2 streams on the oxidizer side while producing highly concentrated, sequestration-ready CO_2 streams on the reducer side. In this case, however, the fraction of CO_2 in the oxidizing stream will impact the temperature rise in the system. This is shown in Fig. 11, where the maximum temperature rise during oxidation with CO_2 is shown again as a function of the FeO weight loading of the carrier for a range of CO_2 mass fractions in the oxidizing feed stream (the balance is assumed to be inert gas). The maximum temperature is only weakly affected by the change in oxidizing gas composition, supporting the feasibility of a CLDR-based process that would be operated with dilute CO_2 feed streams. Beyond offering activation of CO_2 as alternative to CO_2 sequestration, CLDR hence opens the possibility to operate with dilute CO_2 streams (including, potentially, power plant flue gases) that would otherwise require expensive separation for CO_2 concentration before being considered for sequestration.

3. Conclusions

Carbon capture and sequestration is a key element in addressing the challenges posed by climate change. Truly sustainable approaches towards solving the current imbalance in the global carbon cycle, however, should preferentially be built around "carbon reuse" through CO_2 activation and utilization instead of sequestration. In the present work, we proposed and investigated the feasibility of a novel "chemical looping dry reforming" (CLDR) process, which combines CO_2 capture with CO_2 activation in one integrated process. The process is built on the principle of chemical looping combustion (CLC) in which a solid "oxygen carrier" is used as oxygen transfer agent between an oxidant and a fuel. By replacing air with CO_2 as oxidant, CLDR results in the activation of CO_2 via reduction to CO on the oxidizer side of the process, while maintaining the well-established capability of CLC of capturing highly concentrated CO_2 streams without the need for further separation steps.

Using thermodynamic screening calculations, iron-based carriers were identified as the most promising candidates for CLDR, despite limitations in conversion and selectivity in particular when using methane as fuel. Thermogravimetric analysis (TGA) and fixed-bed reactor studies with hydrogen as simple model fuel confirmed the fundamental feasibility of CLDR, using nanostructured Fe–BHA (barium-hexaaluminate) carriers. The carriers showed stable, reproducible cyclic redox behavior with good capacity and fast CO_2 reduction kinetics. Finally, a simplified reactor model for a fixed-bed CLDR process confirmed the feasibility of such a process in a periodically operated fixed-bed configuration, allowing for much more compact and efficient, single-bed processes in comparison to dual circulating fluidized beds, completely avoiding catalyst attrition issues.

The most significant advantage of CLDR over existing alternate processes, however, may lie in its flexibility. By separating the CO_2 reduction and fuel oxidation steps into two separate half-reactions, the process becomes fuel-flexible, i.e. it can in principle be operated with a wide range of fossil and renewable fuels, and it can process highly dilute CO_2 streams as long as the other stream constituents do not negatively interact with the carrier.

Clearly, more detailed analysis of CLDR is required. Efficient operation of such a process will require near-complete conversion of the fuel towards total combustion products. Similarly, CO_2 conversions on the oxidizer side will need further improvement over the result of the present proof-of-principle study. Nevertheless, the results support the fundamental feasibility of the proposed process, and further studies of the detailed oxidation and reduction kinetics of the presented nanostructured carriers with CO_2 and methane, respectively, including the impact of Fe particle size, are currently under way.

Acknowledgements

This technical effort was performed in support of the U.S. Department of Energy's National Energy Technology Laboratory's on-going research under the RDS contract DE-AC26-04NT41817. G.V. gratefully acknowledges support through faculty fellowships from DOE-NETL and from the University of Pittsburgh's Swanson School of Engineering. M.N. gratefully acknowledges support through a GAANN-fellowship from the U.S. Department of Education through the University of Pittsburgh's Mascaro Center for Sustainable Innovation.

References

Akanuma, K., Tabata, M., Hasegawa, N., Tsuji, M., Tamaura, Y., Nakahara, Y., Hoshino, S., 1993. Characterization of carbon deposited from carbon-dioxide on oxygen-deficient magnetites. J. Mater. Chem. 3, 943–946.

Cao, Y., Casenas, B., Pan, W.P., 2006. Investigation of chemical looping combustion by solid fuels. 2. Redox reaction kinetics and product characterization with coal, biomass, and solid waste as solid fuels and CuO as an oxygen carrier. Energy Fuel 20, 1845–1854.

Choudhary, T.V., Choudhary, V.R., 2008. Energy-efficient syngas production through, catalytic oxy-methane reforming reactions. Angew. Chem. Int. Ed. Engl. 47, 1828–1847.

Fan, M.S., Abdullah, A.Z., Bhatia, S., 2009. Catalytic technology for carbon dioxide reforming of methane to synthesis gas. Chemcatchem 1, 192–208.

Glockler, B., Gritsch, A., Morillo, A., Kolios, G., Eigenberger, G., 2004. Autothermal reactor concepts for endothermic fixed-bed reactions. Chem. Eng. Res. Des. 82, 148–159.

Hossain, M.M., de Lasa, H.I., 2008. Chemical-looping combustion (CLC) for inherent CO_2 separations – a review. Chem. Eng. Sci. 63, 4433–4451.

Inoue, H., Sekizawa, K., Eguchi, K., Arai, H., 1997. Preparation of hexa-aluminate catalyst thick films on alpha-SiC substrate for high temperature application. J. Mater. Sci. 32, 4627–4632.

Ishida, M., Jin, H.G., 1994. A new advanced power-generation system using chemical-looping combustion. Energy 19, 415–422.

Kirchhoff, M., Specht, U., Veser, G., 2005. Engineering high-temperature stable nanocomposite materials. Nanotechnology 16, S401–S408.

Kolios, G., Frauhammer, J., Eigenberger, G., 2000. Autothermal fixed-bed reactor concepts. Chem. Eng. Sci. 55, 5945–5967.

Leion, H., Mattisson, T., Lyngfelt, A., 2007. The use of petroleum coke as fuel in chemical-looping combustion. Fuel 86, 1947–1958.

Leion, H., Jerndal, E., Steenari, B.M., Hermansson, S., Israelsson, M., Jansson, E., Johnsson, M., Thunberg, R., Vadenbo, A., Mattisson, T., Lyngfelt, A., 2009. Solid fuels in chemical-looping combustion using oxide scale and unprocessed iron ore as oxygen carriers. Fuel 88, 1945–1954.

Liu, T.F., Temur, H., Veser, G., 2009. Autothermal reforming of methane in a reverse-flow reactor. Chem. Eng. Technol. 32, 1358–1366.

Lyngfelt, A., Leckner, B., Mattisson, T., 2001. A fluidized-bed combustion process with inherent CO_2 separation; application of chemical-looping combustion. Chem. Eng. Sci. 56, 3101–3113.

Mattisson, T., Lyngfelt, A., Cho, P., 2001. The use of iron oxide as an oxygen carrier in chemical-looping combustion of methane with inherent separation of CO_2. Fuel 80, 1953–1962.

Mattisson, T., Garcia-Labiano, F., Kronberger, B., Lyngfelt, A., Adanez, J., Hofbauer, H., 2007. Chemical-looping combustion using syngas as fuel. Int. J. Greenhouse Gas Control 1, 158–169.

Moon, D.J., Ryu, J.W., Lee, S.D., 2004. Carbon dioxide reduction technology with SOFC system. Carbon Dioxide Util. Global Sustainab. 153, 193–196.

Neumann, G., Veser, G., 2005. Catalytic partial oxidation of methane in a reverse flow reactor. AIChE J. 51, 210–223.

Noorman, S., Annaland, M.V., Kuipers, H., 2007. Packed bed reactor technology for chemical-looping combustion. Ind. Eng. Chem. Res. 46, 4212–4220.

Rostrup-Nielsen, J.R., 2002. Syngas in perspective. Catal. Today 71, 243–247.

Ryden, M., Lyngfelt, A., Mattisson, T., 2008. Chemical-looping combustion and chemical-looping reforming in a circulating fluidized-bed reactor using Ni-based oxygen carriers. Energy Fuels 22, 2585–2597.

Solunke, R.D., Veser, G., 2009. Nanocomposite oxygen carriers for chemical-looping combustion of sulfur-contaminated synthesis gas. Energy Fuel 23, 4787–4796.

Solunke, R., Veser, G., 2010. Hydrogen production via chemical looping steam reforming in a periodically operated fixed-bed reactor. Ind. Eng. Chem. Res., doi:10.1021/ie100432j, Article ASAP.

Takenaka, S., Nomura, K., Hanaizumi, N., Otsuka, K., 2005. Storage and formation of pure hydrogen mediated by the redox of modified iron oxides. Appl. Catal. A – Gen. 282, 333–341.

Tamaura, Y., Tabata, M., 1990. Complete reduction of carbon-dioxide to carbon using cation excess magentite. Nature 346, 255–256.

U.S. E.P.A., 2010. Greenhouse Gas Inventory Report.

U.S. E.I.A., 2010. Monthly Energy Review.

Vernon, P.D.F., Green, M.L.H., Cheetham, A.K., Ashcroft, A.T., 1992. Partial oxidation of methane to synthesis gas and carbon-dioxide as an oxidizing agent for methane conversion. Catal. Today 13, 417–426.

Veser, G., 2010. Multiscale process intensification for catalytic partial oxidation of methane: from nanostructured catalysts to integrated reactor concepts. Catal. Today 157, 24–32.

Yamasue, E., Yamaguchi, H., Nakaoku, H., Okumura, H., Ishihara, K.N., 2007. Carbon dioxide reduction into carbon by mechanically milled wustite. J. Mater. Sci. 42, 5196–5202.

Zafar, Q., Mattisson, T., Gevert, B., 2006. Redox investigation of some oxides of transition-state metals Ni, Cu, Fe, and Mn supported on SiO_2 and $MgAl_2O_4$. Energy Fuels 20, 34–44.